Journal of Agrometeorology

(A publication of Association of Agrometeorologists)

ISSN : 0972-1665 (print), 2583-2980 (online)
Vol. No. 27 (3) : 313-319 (September - 2025)
https://doi.org/10.54386/jam.v27i3.2964
https://journal.agrimetassociation.org/index.php/jam

Research Paper

Analysing hydrological balance of Pindar-Nandakini River Basin, Kumaon Himalaya using SWAT model

PANKAJ CHAUHAN[1,2*], KAJAL YADAV[3], NILENDU SINGH[1], RIZWAN AHMAD[4], RAJIB SHAW[5] and HARIS HASAN KHAN[4]

[1]*Wadia Institute of Himalayan Geology, Dehradun, India- 248001*
[2]*Academy of Scientific and Innovative Research (AcSIR), Ghaziabad, India- 201002*
[3]*MDS University, Ajmer, Rajasthan- 305009, India*
[4]*Interdisciplinary Department of Remote, Sensing and GIS Applications, Aligarh Muslim University, Aligarh 202001, Uttarpradesh*
[5]*Graduate School of Media and Governance, Keio University, 5322 Endo, Fujisawa 252-0882, Kanagawa, Japan*
[*]*Corresponding author Email: Pchauhan1008@gmail.com*

ABSTRACT

Water availability from the central Himalayan River Basins is threatened by warming-mediated glacier melt and declining precipitation. This study employed the Soil and Water Assessment Tool (SWAT) model to analyze the water balance of the Pindar-Nandakini River Basin (PRB). The model was calibrated and validated using high-resolution data, achieving strong performance (R^2: 0.85, NSE: 0.71). Runoff and evapotranspiration (ET) account for approximately 29.7% and 28.9% respectively. Lateral soil flow is a major contributor (23.7% of precipitation), significantly influencing streamflow and groundwater levels. Snowmelt contributes around 10.3%, while deep groundwater flow is minimal. The model considerably simulated seasonal runoff patterns, particularly peak flows during the monsoon. Sediment loading, at 563.1 t ha^{-1} annually, is a significant concern. The study also underscores the critical role of ET and runoff in the hydrological processes of the basins, revealing potential challenges during high-flow events and climate-driven forest greening trends. These findings emphasize the importance of the SWAT model in understanding the complex hydrological processes within the Himalayan glacier basins, highlighting the basin's vulnerability to climate change impacts, particularly glacier retreat.

Keywords: SWAT modelling, Glacier valleys, Pindar-Nandakini River Basin, Groundwater recharge; Central Himalaya

The reduction in glacier extent and the declining trend in precipitation will lead to decreased water availability downstream. The role of mountain hydrology is extensive and hydrologically significant, and it has experienced notable decreasing flow trends for several years (Lizama *et al.,* 2024). The Himalayas are a vital source of water for millions, and they are under increasing pressure from human activities and climate change. A severe lack of studies on the region's water balance hinders efforts to manage water resources effectively and prepare for disasters. The Pindar-Nandakini River Basin (PRB), located in the Kumaun Himalaya (Uttarakhand), is a water source for agriculture, hydropower, and drinking water. However, this vital resource is under increasing pressure due to climate change, population growth, and land-use changes (Chauhan *et al.,* 2022; Singh *et al.,* 2013; Singh *et al.,* 2020). Understanding this basin's complex water flow dynamics and availability is essential for future sustainability. This study employs the widely used SWAT model (Soil and Water Assessment Tool) to simulate the Pindar-Nandakini River Basin (PRB) water balance and runoff dynamics.

In the last few decades, several watershed analysis models have been introduced, including SWAT, APEX, HSPF, WAM, KINEROS, and MIKE-SHE. Each model varies in terms of required input data and structural complexity (Arnold *et al.,* 2015; Moriasi *et al.,* 2007). The SWAT model operates through the ArcSWAT interface, leveraging ArcGIS for geographical analyses

Article info - DOI: *https://doi.org/10.54386/jam.v27i3.2964*
Received:12 March 2025; Accepted: 9 May 2025; Published online : 1 September 2025

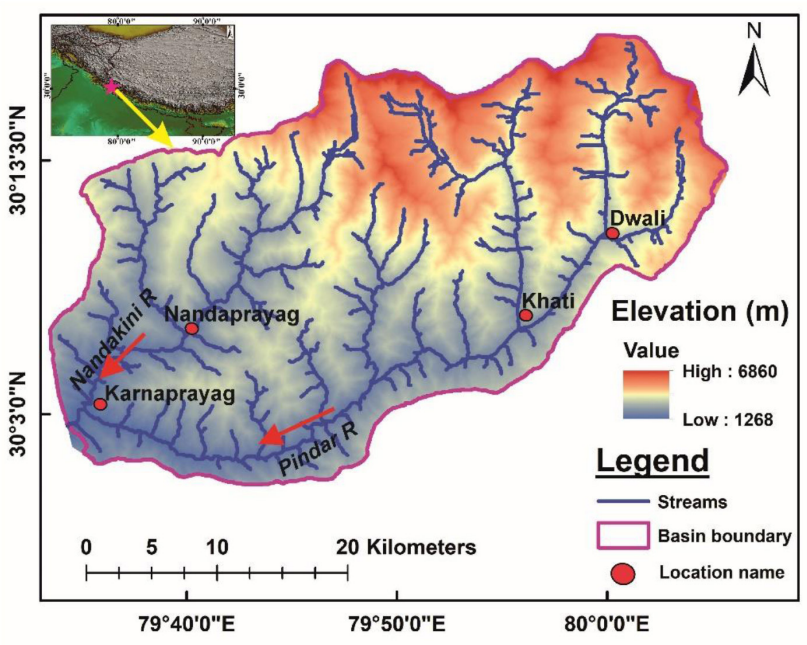

Fig. 1: Location map of the study area

that feed into the SWAT framework to generate hydrological data. The SWAT model has widespread adoption and effectiveness in various studies (Londhe and Katpatal, 2020; Thakuri and Salerno, 2016; Suryavanshi *et al.,* 2017; Koltsida *et al.,* 2023; Padhiary *et al.,* 2018; Rank *et al.,* 2023).

In this study, the SWAT model has been employed to assess and quantify the seasonal water balance in the study basins, leveraging the availability of monthly streamflow data. Present study aimed to rigorously calibrate, validate, and assess the SWAT model's capability to analyze water balance components specific to the conditions of the study basins in the Himalayan region.

MATERIAL AND METHODS

Study area

The area of interest includes the Nandakini and the Pindar basin that covers an area of ~ 110589.4 ha and stretches between 30°N to 18°N latitude and 79°13' to 80°E longitude up to the Karnaprayag (Fig. 1). It occupies the eastern region of the Kumaun Himalaya, with elevations ranging from 800 to 6,800 meters. Pindari (11100 ha) and Kafni (6200 ha) are the contiguous glacier basins in within the study area and drain a total area of about 173 km^2 up to Dwali and constitute a significant part of Pindar valley in Uttarakhand state (Chauhan *et al.,* 2023). Nandakini and Pindari are the main tributaries of the Alaknanda River. The Nandakini river originates from the Nanda Ghughati peak and merges with the Alaknanda at Nandaprayag.

Data sets

The SWAT model utilizes several datasets, including a digital elevation model (DEM), land use maps, soil maps, and various meteorological parameters. Table 1 summarises input data and their respective sources utilized in this analysis. A 30 m resolution DEM was acquired from the U.S. Geological Survey (USGS) website. The land use map, based on the 30 m resolution 2021 CORINE Land Cover (CLC) data, was adjusted to fit the SWAT model's land use categories (Table 2). Soil information was sourced from the Food and Agriculture Organization's Digital Soil Map of the World (www. Fao.org). Meteorological inputs such as rainfall, relative humidity, wind speed, and daily minimum and maximum temperatures were collected from the Power Data Access Viewer (https://power.larc.nasa.gov/data-access-viewer). Additionally, solar radiation and other weather data were generated by weather generator (WGEN) module designed by SWAT that uses monthly statistics to estimate missing meteorological data. This study used MODIS ET data for validation of the results.

Soil water assessment tool (SWAT) model

The SWAT simulation process begins with watershed delineation, where the watershed is divided into sub-basins based on topography and hydrological characteristics. Each sub-basin is further subdivided into Hydrologic Response Units (HRUs), defined by unique land use combinations, soil type, and slope. This segmentation allows the model to capture spatial variability in hydrological processes across the watershed (Arnold *et al.,* 2013; Neitsch *et al.,* 2011). This involves gathering meteorological data (precipitation, temperature, solar radiation, wind speed, and humidity), land use and land cover maps, soil properties (texture, depth, and hydraulic conductivity), topographic data from a Digital Elevation Model (DEM), and details of agricultural management practices like irrigation and fertilization. Accurate and comprehensive data are essential to ensure reliable simulation results (Gassman *et al.,* 2007). The HRUs are distinguished by unique combinations of soil type, slope, and land use, allowing the model to capture variations in evapotranspiration across different vegetation and soil conditions. The model processes hydrological dynamics in two main phases: the land phase, which calculates how much water, sediment, nutrients,

Table 1: Data sources used in SWAT model

Data type	Resolution	Sources	Description
DEM	30 m	Shuttle Radar Topography Mission (https://earthexplorer.usgs.gov/)	Digital Elevation Model
Land Use	30 m	Corine land cover	Land Use Map
Soil	30 Arcs (1:5000000)	food and agriculture organization (https://www.fao.org/home/en/)	Soil Map
Weather Data	-	Power Data Access Viewer (https://power.larc.nasa.gov/data-access-viewer)	Precipitation, minimum and maximum air temperatures, relative humidity, wind speed
MODIS/Terra Net Evapotranspiration	500 m	EARTHDATA	Evapotranspiration (ET)

Table 2: Land use classification of the basin and the corresponding SWAT land use category

CLC Code	CORINE description	SWAT code	SWAT description	Watershed (%)
122	Road and rail networks and associated land	UTRN	Transportation	0.2
112	Discontinuous urban fabric	URLD	Residential – low density	4.4
		ALMD	Almond	0.2
		BANA	Banana	37.9
		SWCH	Switchgrass	0.0
		COCB	Cocoa beans	20.3
		CASS	Cassava	0.0
24		UINS	Urban Institutional	36.9

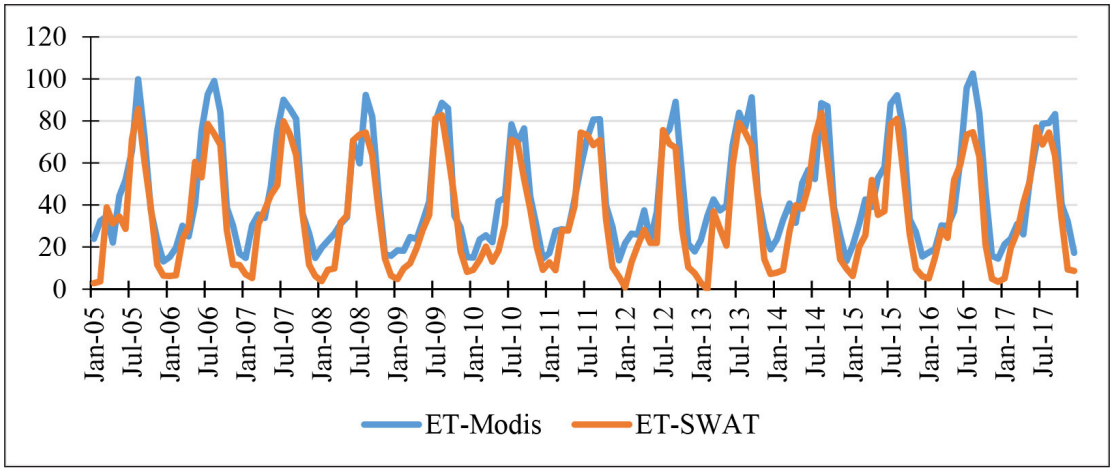

Fig. 2: Comparison of SWAT-simulated vs. MODIS evapotranspiration data (in mm).

and pesticides are delivered to stream channels, and the routing phase, which simulates the movement of these elements through the stream network to the basin outlet (Neitsch *et al.,* 2011). Each HRUs independently simulates hydrological processes including canopy storage, surface runoff, precipitation partitioning, soil water infiltration and redistribution, evapotranspiration, lateral subsurface flow, and return flow from shallow aquifers (Gassman *et al.,* 2007). The model was evaluated using statistical performance measures such as correlation coefficient (r), coefficient of determination (R^2) and Nash-Sutcliffe Efficiency (NSE).

RESULTS AND DISCUSSION

SWAT calibration and validation

The model calibration yielded a correlation coefficient (r = 0.92), reflecting a high correlation between observed and simulated streamflow, which suggests effective parameter tuning. The coefficient of determination (R^2 = 0.85), meaning the model captured 85% of the observed streamflow variability, indicating a strong model fit. The Nash-Sutcliffe Efficiency (NSE) for calibration was 0.71, close to the optimal value of 1, confirming the model's effectiveness in replicating observed streamflow trends with minimal error. The accompanying graph (Fig. 2) compares SWAT-simulated evapotranspiration (ET) with MODIS-observed ET values from 2005 to 2017. It shows that the SWAT model effectively captures the seasonal evapotranspiration trends, with minor deviations from MODIS data, further confirming the model's accuracy during calibration. In the validation phase, the R-value remained high during validation, reflecting a strong correlation between simulated and observed streamflow values. The R^2 value

Table 3: Detailed characteristics of HRU's, land-use, soil and slope used in SWAT simulation

Land-use category	**Class**	**Area (ha)**	**Watershed area (%)**
Residential-Low Density	URLD	1169.0	1.1
Cockle Burr	COCB	23270.2	21.0
Bananas	BANA	42968.6	38.9
Institutional	UINS	43181.6	39.0
Soil category	**Class**		
Loam	I-Bh-U-C-3717	95722.2	86.6
Clay loam	Bd29-3C-3661	14867.2	13.4
Slope	**Slope class (%)**		
1	99-45	101424.1	91.7
2	45-30	8581.8	7.8
3	30-15	295.8	0.3
4	15-0	287.7	0.3

Table 4: SWAT simulated monthly values of hydrological parameters

Month	Rain (mm)	Snow fall (mm)	Surface water (mm)	Lateral soil flow (mm)	Water yield (mm)	ET (mm)	Sediment yield (t ha^{-1})	PET (mm)
January	33.3	32.6	1.9	2.6	6.3	5.1	1.0	12.2
February	49.0	48.9	8.3	11.6	21.9	7.2	7.7	11.2
March	13.7	7.6	4.9	7.9	20.1	15.8	32.6	42.6
April	15.6	0.8	0.9	2.6	10.2	16.2	3.4	65.4
May	27.1	0.0	3.0	3.9	10.3	19.2	14.5	88.1
June	134.3	0.0	52.4	23.9	77.7	34.9	251.2	87.7
July	286.7	0.0	87.9	67.5	165.3	56.8	117.6	76.8
August	279.1	0.0	88.3	77.8	183.2	61.6	73.0	75.0
September	183.0	0.0	62.4	46.9	157.6	48.2	60.3	66.0
October	11.2	0.0	0.6	2.6	39.2	23.3	0.8	55.1
November	6.7	2.1	0.5	1.1	19.2	10.0	0.7	34.8
December	9.9	15.7	0.4	0.8	7.9	5.2	0.2	22.3
Annual	1049.6	107.7	311.4	249.1	718.9	303.4	563.1	637.1

also stayed within an acceptable range, confirming that the model continued to explain most of the variance in observed data during validation.

Hydrologic response units (HRUs)

Hydrologic response units (HRUs) used in the SWAT model simulation conducted on October 4, 2023. This simulation uses thresholds of 12%, 15%, and 15% for land use, soil, and slope, respectively, which ensures that only areas above these values are included in HRU creation, reducing model complexity by excluding minor land features. The watershed covers a total area of 110,589.4 hectares, with specific distributions across land use, soil type, and slope categories. The primary land uses are Institutional (UINS) and Banana (BANA) plantations, which together account for nearly 78% of the watershed, covering 43,181.6 ha (39.0%), 42,968.6 ha (38.9%), respectively. A detailed characteristics of the HRUs, land-use, soil and slope is shown in Table 3.

Other notable land uses include Cockle Burr (COCB) at 21.0% of the area and Residential-Low Density (URLD) at 1.1%. The watershed's soil composition is dominated by two type of soil Loam: "I-Bh-U-c-3717," which covers 95,722.2 ha (86.6%), with the secondary soil type, Clay loam: "Bd29-3c-3661," occupying 14,867.2 ha (13.4%). Slope analysis reveals that a significant portion of the watershed (91.7%) consists of steep slopes (99-45%), while gentler slopes between 45-30% comprise a smaller fraction. This distribution of steep slopes indicates a potential for higher runoff and erosion within the watershed.

Precipitation and snow dynamics

The basins receives an average annual precipitation of approximately 1049.6 mm, with snowfall contributing around 107.7 mm or about 10.3% of the total. The snow completely melts by spring, contributing directly to runoff and infiltration without significant sublimation. This absence of sublimation suggests a

Table 5: Characteristics of basin and hydrological parameters simulated from SWAT

Characteristics parameters	Values	Characteristics parameters	Values
General watershed detail		***Hydrological parameters***	
Watershed area (ha)	110589.4	Precipitation (mm)	1049.6
Sub-basins	7	Snow fall (mm)	107.7
Number of HRUs	26	Snow melt (mm)	107.7
Water stress days		Sublimation (mm)	0
Water stress days	9.6	Surface runoff: (mm)	311.4
Temperature stress days	148.5	Lateral soil flow: (mm)	249.1
Nitrogen stress days	32.3	Return flow	149.5
Phosphorus stress days	0.1	Tile: (mm)	0
Aeration stress days	0	Ground water (shallow): (mm)	142.7
Hydrology (water balance ratio)		Ground water (Deep): (mm)	6.8
Stream flow/ precipitation	0.68	Evaporation (mm)	12.7
Base flow/Total flow	0.56	Deep AQ Recharge (mm)	8.6
Surface flow/Total flow	0.44	Total AQ Recharge (mm)	167.3
Percolation/Precipitation	0.16	Total water yield (mm)	718.9
Deep recharge/Precipitation	0.01	Percolation out of soil (mm)	172.4
ET/ Precipitation	0.29	ET (mm)	303.4
Stream flow/ precipitation	0.68	PET (mm)	637.1
Stream flow/ precipitation	0.68	Total sediment loading (tha^{-1})	563.1

temperate climate that allows snow to transition smoothly into the watershed's hydrological system. Seasonal patterns reveal that the highest rainfall occurs in July, with about 286.7 mm nearly 27.3% of the total annual precipitation. Snowfall primarily occurs in winter, peaking in January (32.6 mm) and February (48.9 mm), accounting for 30.2% and 45.4% of total snowfall, respectively (Table 4). The concentration of precipitation in July in the basin mirrors monsoon-driven rainfall patterns seen throughout the Himalaya, where the monsoon season can account for over 50% of annual total. However, the impact of the monsoon is comparatively moderate in our study region, likely due to its temperate climate and elevation, which reduce the intensity of monsoon rainfall relative to lower-altitude regions. Additionally, snowmelt, which accounts for 10% of annual precipitation, provides critical water input in early summer, supporting water availability during drier months.

Runoff and soil water dynamics

Surface runoff is a critical component of the watershed's hydrology, averaging 311.4 mm annually. Surface runoff is highest during the monsoon months, with July (87.9 mm) and August (88.3 mm) contributing significantly. This high runoff during summer is likely due to intense rainfall events, which leads to increased stream flow, influencing flood risks and water availability downstream. Lateral soil flow, which represents the horizontal movement of water through the soil towards water bodies, averages 249.1 mm annually, this flow is significant in maintaining streamflow and groundwater recharge. The highest lateral soil flow occurs in August (77.8 mm) and July (67.5 mm), aligning with the peak rainfall months, indicating that the soil has good infiltration capacity and allows for substantial lateral movement of water, the detailed statistics is presented in (Table 4). This suggests minimal human intervention in water movement, preserving the natural hydrological processes and supporting a balanced water cycle.

Groundwater flow

Groundwater flow is divided into contributions from shallow and deep aquifers. The shallow deep aquifer provides 142.7 mm annually, while the deep aquifer contributes 6.8 mm. This highlights the importance of the shallow aquifer in sustaining groundwater flow and maintaining base flow in streams in the basin. The evaporation process, where water from the shallow aquifer returns to the soil and plants, is 12.7 mm annually (Table 5). This is crucial for maintaining soil moisture and supporting vegetation, particularly during dry periods. Deep aquifer recharge occurs at 8.6 mm annually, contributing to the total aquifer recharge of 167.3 mm. This indicates that a significant portion of infiltrated water replenishes the aquifers, underscoring the importance of groundwater in mountain watershed hydrology. Therefore, we contend that effective groundwater management is essential to ensure sustainable water supplies and support ecosystem health particularly during dry season.

Recharge, yield and Evapotranspiration

The total water yield, encompassing surface runoff, lateral soil flow, and groundwater flow, is 718.9 mm annually. The percolation out of the soil is 172.4 mm annually, indicating the

downward movement of water through the soil profile to replenish deeper groundwater layers. This process is vital for sustaining long-term groundwater supplies and maintaining the hydrological balance. Actual evapotranspiration (ET), which combines evaporation and plant transpiration, averages 303.4 mm annually (Table 4). This value reflects the actual water loss to the atmosphere from the soil and vegetation. Potential evapotranspiration (PET) is higher at 637.1 mm, indicating the amount of evaporation that could occur with optimal water and vegetation cover. The difference between PET and ET (333.7 mm) suggests that the limited water availability restricts actual evapotranspiration, a critical factor in understanding water demand versus supply in the given ecosystem. Monthly ET values peak in July (56.8 mm) and August (61.6 mm), corresponding with the highest rainfall and temperature periods (Table 4). Efficient water management practices are essential to meet this demand, particularly for the agriculture.

Sediment loading, other losses and Stress days

Total sediment loading, recorded at 563.1 t ha^{-1}, measures the amount of sediment transported by runoff (Table 5). Very high sediment loading indicates significant soil erosion, which can degrade soil quality and impact water quality downstream. The highest sediment yields occur in June (251.2 t ha^{-1}), July (117.6 t ha^{-1}), and August (73.00 t ha^{-1}), coinciding with peak runoff periods (Table 4). Addressing sediment loading is essential for soil conservation and maintaining water quality. The watershed experiences an average water and temperature stress days as 9.6 and 48.5 respectively in the basin annually (Table 5), indicating periods when water availability is insufficient to meet demand. Temperature stress days reflecting periods of extreme temperatures that can affect plant growth and water usage. Nitrogen stress days average 32.3 annually, highlighting nutrient limitations that can impact agricultural productivity. Phosphorus and aeration stress days are negligible, indicating that these factors are not significant limitations in this watershed, the detailed SWAT simulation results are presented in (Table 4 and 5).

CONCLUSIONS

The SWAT model outputs reveals that the precipitation and snowmelt are vital contributors to the water balance of Pindar-Nandakini River Basin. Surface runoff, averaged annually peaks during the monsoon months, reflecting the basin's response to intense rainfall events. Similarly, the substantial lateral soil flow indicates the basin's good infiltration capacity and its crucial role in maintaining streamflow and groundwater recharge. Groundwater flow, particularly from the shallow aquifer. This underscores the importance of shallow aquifers in sustaining base flows and supporting overall water availability. The study also reveals a significant gap between actual evapotranspiration and potential evapotranspiration annually. The basin faces considerable sediment loading, with peaks during high runoff periods. Furthermore, the basin experiences an average water and temperature stress days annually, highlighting periods of insufficient water availability and extreme temperatures that can adversely affect plant growth and water usage. This study underscores the importance of advanced hydrological modeling tools in informing effective water resource management strategies in complex geographical settings as well as key areas or hydrological processes crucial for conservation or integrated management efforts in the Himalayan glacier regions.

ACKNOWLEDGEMENT

The authors are thankful to the Director, Wadia Institute of Himalayan Geology (WIHG), for all logistical support.

Sources of Funding: This study was not funded.

Conflict of Interest Statement: The author(s) declare(s) that there is no conflict of interest.

Data Availability Statement: Data to be provided on request.

Author's contributions: **P Chauhan and K Yadav**: Conceptualization, Methodology, Data curation editing; **N Singh and R Ahmad:** Methodology, Visualization; **R Shaw:** Formal analysis, Writing-original draft; Supervision; **HH Khan:** Writing-review and editing

REFERENCES

Arnold, J.G., Moriasi, D.N., Gassman, P.W., Abbaspour, K.C., White, M.J., Srinivasan, R. and Kannan, N. (2013). SWAT: model use, calibration, and validation. *Trans. ASABE* 55 (4): 1491-1508.

Arnold, J.G., Youssef, M.A., Yen, H., White, M.J., Sheshukov, A.Y., Sadeghi, A.M., Moriasi, D.N., Steiner, J.L., Amatya, D.M., Skaggs, R.W. and Haney, E.B. (2015). Hydrological processes and model representation: impact of soft data on calibration. *Trans. ASABE*, 58(6):1637-1660.

Chauhan, P., Akıner, M.E., Sain, K. and Kumar, A. (2022). Forecasting of suspended sediment concentration in the Pindari-Kafni glacier valley in Central Himalayan region considering the impact of precipitation: using soft computing approach. *Arab. J. Geosci.,* 15(8):683.

Chauhan, P., Sharma, J., Bhardwaj, P., Mehta, M., Shah, R.A., Singh, O. and Sain, K. (2023). Comparative analysis of discharge and sediment flux from two contiguous glacierized basins of Central Himalaya, India. *Environ. Monit. Assess,* 195(6):729.

Gassman, P.W., M. R. Reyes, C. H. Green, and J. G. Arnold. (2007). The Soil and Water Assessment Tool: Historical development, applications, and future research directions. *Trans. ASABE*, 50(4): 1211-1250. doi:10.13031/2013.23637.

Koltsida, E., Mamassis, N. and Kallioras, A. (2023). Hydrological

modeling using the Soil and Water Assessment Tool in urban and peri-urban environments: the case of Kifisos experimental subbasin (Athens, Greece). *Hydrol. Earth Syst. Sci.,* 27(4): 917-931.

Lizama, E., Somos-Valenzuela, M., Rivera, D., Lillo, M., Morales, B., Baraër, M. and Fernández, A. (2024). Role of mountain glaciers in the hydrological dynamics of headwater basins in the Wet Andes. *J. Hydrol.,* 649:132413.

Londhe, D.S. and Katpatal, Y.B. (2020). Comparative assessment of evapotranspiration in Bhima sub-basin using spatial analysis for normal and ENSO years. *J. Agrometeorol.,* 22(2): 179-185. https://doi.org/10.54386/jam.v22i2.159

Moriasi, D.N., Arnold, J.G., Van Liew, M.W., Bingner, R.L., Harmel, R.D. and Veith, T.L. (2007). Model Evaluation Guidelines for Systematic Quantification of Accuracy in Watershed Simulations. *Trans. ASABE* 50, 885-900.

Neitsch, S.L., Arnold, J.G., Kiniry, J.R. and Williams, J.R. (2011). Soil and water assessment tool theoretical documentation version 2009. Texas Water Resources Institute Technical report no. 406, Texas A&M University, Texas.

Padhiary, J., Patra, K.C., Das, D.M., Sahoo, B.C. and Singh, K.K. (2018). Prediction of climate change impact on streamflow and evapotranspiration in Baitarani basin using SWAT model. *J. Agrometeorol.,* 20(4): 325-328. https://doi.org/10.54386/jam.v20i4.576

Rank, P.H., Vaghasiya, D.R., Lunagaria, M.M., Patel, R.J., Tiwari, M.K. and Rank, H.D. (2023). Climate change impacts on water flux dynamics in Shingoda basin having agriculture and forest ecosystems: A comprehensive analysis. *J. Agrometeorol.,* 25(3): 397-403. https://doi.org/10.54386/jam.v25i3.2284

Singh, N., Bhattacharya, B. K., Soni, P., Raja, P., Singh, M.P. and Parihar, J. S. (2013). Energy and Water Dynamics Over Young Pine Forest as Influenced by Climatic Variability and Land Management Practices. *J. Agrometeorol.,* 15(Special issue): 100-107.

Singh, N., Singhal, M., Chhikara, S., Karakoti, I., Chauhan, P. and Dobhal, D.P. (2020). Radiation and energy balance dynamics over a rapidly receding glacier in the central Himalaya. *Int. J. Climatol.,* 40(1):.400-420.

Suryavanshi, S., Pandey, A. and Chaube, U. C. (2017). Hydrological simulation of the Betwa River basin (India) using the SWAT model. *Hydrol. Sci. J.,* 62(6): 960-978.

Thakuri, S., and Salerno, F. (2016). Glacio-hydrological simulation in Dudh Koshi River basin, Nepal. *Intern. J. Sci. Develop. Res.,* (*IJSDR)*, 1:72-78.